*10098–10105* *Nucleic Acids Research, 2021, Vol. 49, No. 17* *Published online 9 September 2021*
*https://doi.org/10.1093/nar/gkab797*

# Nano-sandwich composite by kinetic trapping assembly from protein and nucleic acid

**Shi Chen[3], Li Xing[4], Douglas Zhang[1], Alba Monferrer[1] and Thomas Hermann[1,2,*]**

[1]Department of Chemistry and Biochemistry, University of California, San Diego, 9500 Gilman Drive, La Jolla, CA 92093, USA, [2]Center for Drug Discovery Innovation, University of California, San Diego, 9500 Gilman Drive, La Jolla, CA 92093, USA, [3]Materials Science and Engineering Program, University of California, San Diego, 9500 Gilman Drive, La Jolla, CA 92093, USA and [4]Irvine Materials Research Institute, University of California, Irvine, CA 92697, USA

Received May 17, 2021; Revised August 06, 2021; Editorial Decision August 31, 2021; Accepted September 08, 2021

## ABSTRACT

**Design and preparation of layered composite materials alternating between nucleic acids and proteins has been elusive due to limitations in occurrence and geometry of interaction sites in natural biomolecules. We report the design and kinetically controlled stepwise synthesis of a nano-sandwich composite by programmed noncovalent association of protein, DNA and RNA modules. A homo-tetramer protein core was introduced to control the self-assembly and precise positioning of two RNA–DNA hybrid nanotriangles in a co-parallel sandwich arrangement. Kinetically favored self-assembly of the circularly closed nanostructures at the protein was driven by the intrinsic fast folding ability of RNA corner modules which were added to precursor complex of DNA bound to the protein. The 3D architecture of this first synthetic protein–RNA–DNA complex was confirmed by fluorescence labeling and cryo-electron microscopy studies. The synthesis strategy for the nano-sandwich composite provides a general blueprint for controlled noncovalent assembly of complex supramolecular architectures from protein, DNA and RNA components, which expand the design repertoire for bottom-up preparation of layered biomaterials.**

## INTRODUCTION

Self-assembling soft materials have been obtained from design and synthesis efforts at the interface of supramolecular chemistry and nanotechnology. The association of molecular building blocks through noncovalent interactions orchestrated by self-recognition leads to materials that exhibit diverse functionality and patterns at nanoscale feature size. Proteins and nucleic acids have unique 3D folding and sequence-encoding properties that render these biopolymers ideal modules for self-assembling soft materials. Proteins provide a diverse repertoire of 3D architectures, chemical functionality and enzymatic activities, while DNA and RNA enable programmable noncovalent assembly through predictable base pair formation. Among nucleic acid components, RNA combines architectural complexity of stable autonomous folds with the ability to assemble in a sequence-dependent fashion (1–3). The three types of biopolymers, proteins, DNA and RNA have been extensively used for nanoscale self-assembly of soft materials with a multitude of applications, for example, in sensing, imaging, catalysis, plasmonic devices, biocompatible coatings, synthetic pores, surface patterning and dynamic nanodevices (4–7). Combining different biopolymer types enables the design of composite materials with increasingly complex properties and functionality at the nanoscale (8). Composite biopolymer nanomaterials have been created from DNA–protein (9–11) and RNA–protein complexes (12,13) as well as RNA–DNA hybrid assemblies (14–18); however, self-assembling materials containing protein and both types of nucleic acid have been elusive to date. Further, while previous efforts to develop composite nanomaterials had succeeded in the controlled placement of proteins on pre-formed DNA or RNA scaffolds (8,10–13), the self-assembly of nucleic acid nanostructures at a protein core remains an unmet challenge of biomolecular nanotechnology.

Molecular complexity in such noncovalent supramolecular systems emerges from precisely vectored assembly rather than inherent chemical complexity of the diverse building blocks. Maximizing control over the preparation of composite materials from multiple different types of biopolymers requires multistep noncovalent synthesis that exploits thermodynamics and kinetics of self-assembly pathways to sequentially process information stored in the constituent component architectures towards creation of the desired

*To whom correspondence should be addressed. Tel: +1 858 534 4467; Fax: +1 858 534 0202; Email: tch@ucsd.edu
Present address: Alba Monferrer, Physics Department, Technische Universität München, Garching, Germany.

complex product (19). Base-pair formation of complementary sequences within nucleic acid building blocks often drives assembly to thermodynamically stable structures which may not be kinetically favored over uncontrolled aggregation. One approach to overcome undesirable pathways of nucleic acid folding and assembly is to exploit local interactions that drive fast folding as a kinetic trap (20), thus avoiding unwanted oligomerization of modules.

Here, we describe the design, stepwise synthesis and structure characterization of a nano-sandwich composite that contains three types of biopolymers, protein, DNA and RNA, each playing a distinct and essential role for assembly and architecture. The composite includes a protein core sandwiched between two co-parallel nanotriangles that assemble from RNA-corner and DNA-connector modules (Figure 1A). Distinct from previous approaches of locating proteins on pre-formed nucleic acid frameworks (10,21,22), we used a protein component to direct self-assembly of nucleic acid nanoshapes in precisely pre-determined positions of a sandwich architecture. As a protein core, we chose streptavidin which is a homo-tetramer of subunits, each containing a high-affinity binding site for a biotin molecule. Association of the nucleic acid nanotriangles with the protein was achieved by DNA oligonucleotide components that carried a biotin ligand.

## MATERIALS AND METHODS

### Materials

DNA and RNA oligonucleotides were purchased from Integrated DNA Technologies. Unmodified DNA and RNA oligonucleotides and biotin-modified DNA oligonucleotides were rehydrated in 10 mM sodium cacodylate buffer, pH 6.5, to 500 μM stock before further diluting to working concentration with the same buffer. Cy5-modified RNA oligonucleotide was dissolved in 10 mM HEPES buffer, pH 7.0, to stock concentration at 200 μM. Oligonucleotide sequences are listed in Supplementary Table S1.

Streptavidin tetramer was purchased from Promega Corporation. Alexa Fluor 488-conjugated streptavidin was purchased from Thermo Fisher Scientific. The protein batch used for the fluorescence experiments described here contained four fluorophores conjugated to streptavidin. Proteins were rehydrated and diluted in 10 mM HEPES buffer, pH 7.0.

### Assembly of RNA–DNA hybrid nanoshapes

RNA–DNA hybrid nanoshapes were assembled by mixing stoichiometric amounts of nucleic acid components and annealing at 37°C for 10 min in the presence of 2 mM magnesium chloride. After annealing, samples were cooled on water ice for 5 min before using for gel electrophoresis analysis.

### Assembly of RNA–DNA–protein composite material

RNA–DNA–protein was assembled in a multi-step protocol in the presence of 2 mM magnesium chloride: (i) streptavidin and biotin-conjugated $DNA_{out}$ connector were mixed at a given ratio and incubated at 37°C for 1 h before cooling on ice for 5 min; (ii) to the mixture were added guide $DNA_{in}$ and unmodified $DNA_{out}$ connector followed by incubation at 37°C for 10 min; (iii) RNA corner module oligonucleotides were added to the mixture and incubated 37°C for 50 min before cooling on water ice for 5 min.

### Native polyacrylamide gel electrophoresis (PAGE)

Nucleic acid assemblies and composite material were analyzed on 5% native acrylamide/bisacrylamide (19:1) gels in 2× MOPS buffer (40 mM 3-morpholinopropane-1-sulfonic acid, 10 mM sodium acetate) containing 2 mM magnesium chloride. Gel electrophoresis was performed at 220 V at 22 mA for 60–90 min.

### Gel extraction

Gel-purified nano-sandwich composite was isolated by extraction from gel slices cut out around the individual band containing the composite after PAGE. The extracted band was cut into small pieces before soaking in 500 μl of 10 mM sodium cacodylate buffer containing 2 mM magnesium chloride at 4°C for 5–7 days. Recovered solutions were concentrated on Amicon ultra 0.5 ml centrifugal filters (regenerated cellulose, 3000 NMWL).

### FRET experiments

FRET experiments were performed as described previously (23) on a Spectra Max Gemini monochromator plate reader (Molecular Devices) at room temperature. Cy5-modified RNA was at 100 nM concentration and Alexa Fluor 488-conjugated streptavidin was at 13.2 nM in 10 mM HEPES buffer (pH 7.0). Alexa Fluor 488 was excited at 480 nm, and transferred fluorescence was read as Cy5 emission at 670 nm. Emission blocking filter was set at 665 nm.

### AFM imaging

Freshly cleaved mica was modified with 50 mM solution of 1-(3-aminopropyl)-silatrane (APS) in deionized water by immersing strips for 30 min followed by rinsing with deionized water and drying in an Ar stream (24). Nucleic acid and composite samples were diluted at 4°C in assembly buffer (10 mM sodium cacodylate buffer, pH 6.5, for nucleic acid samples and 10 mM HEPES, pH 7.0, for sandwich composite) containing 2 mM magnesium chloride and immediately deposited onto APS-modified mica for 2 min. Typical sample concentration for deposition was 0.5–1.5 ng/μl. Samples were rinsed briefly with several drops of ice-cold water and dried with a gentle flow of argon. AFM images were collected with a MultiMode AFM Nanoscope IV system (Bruker Instruments) in Tapping Mode at ambient conditions. Silicon probes RTESPA-300 (Bruker Nano Inc.) with a resonance frequency of ∼300 kHz and a spring constant of ∼40 N/m were used for imaging at scanning rate of about 2.0 Hz. Images were processed using the FemtoScan software package (Advanced Technologies Center).

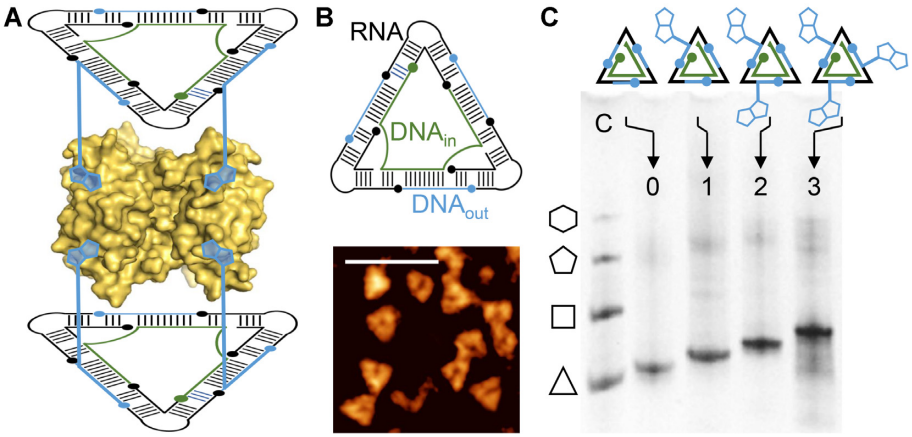


**Figure 1.** Design of nucleic acid-protein nano-sandwich composite. (**A**) Architecture of the nano-sandwich composite containing a streptavidin protein tetramer (yellow) that associates with two flanking nucleic acid nanotriangles, each bound through two DNA-conjugated biotin ligands (blue). The rotational arrangement of the nanotriangles in this and the following schematics is arbitrarily shown in an eclipsed configuration. The design of the nano-sandwich components allows for eclipsed or staggered arrangement. (**B**) Nucleic acid hybrid nanotriangles that self-assemble from RNA corner modules and DNA connectors ($DNA_{out}$) controlled by a DNA guide strand ($DNA_{in}$) with three hybridization sites for the connector units. AFM imaging confirmed the nanotriangle architecture (14). (**C**) Programmed assembly of modified nucleic acid nanotriangles that carry 0–3 biotin ligands attached at DNA connectors ($DNA_{out}$). Increasing number of biotin ligands is revealed by decreasing mobility of modified nanotriangles on native polyacrylamide gel. Lane C is a mobility control sample containing a previously established mixture of unmodified polygonal RNA–DNA hybrid nanoshapes (14).

### Cryo-TEM

Sample vitrification was performed with a Leica EMGP plunger (Leica Microsystems). Briefly, 3 ul of purified sandwich sample was applied to a glow-discharged Quantifoil grid (R1.2/1.3, Electron Microscopy Sciences). The grid was quickly plunged into liquid propane after 3.5 s blotting time at 95% humidity. Specimen was then transferred onto a Gatan cryo-transfer holder (Gatan) and examined under a JEM2100F electron microscope (JEOL USA) with operation voltage at 200 kV. The images were recorded at electron dose $<20$ e/Å$^2$ and collected on a Gatan OneView CCD detector at pixel size of 2.8 Å at specimen space.

### Single particle image processing and 3D reconstruction

Cryo-EM CCD images were processed in cryoSPARC (Structura Biotechnology). After CTF correction, a total of 40764 particles were selected and 2D-classified for *ab-initio* initial models building under C1 symmetry. The initial model with three-layers density distribution was visually selected for further 3D refinements. The final density map was reconstructed by combining 6872 particles under superimposed D3 or C1 symmetry (Supplementary Figure S4). The density consistency for the final maps was calculated to be 5.79 Å by the GSFSC curve without any mask in cryoSPARC. A cryo-EM map for the nano-sandwich composite (Figure 4D) was deposited with the Electron Microscopy Data Bank, EMDB accession code EMD-24824.

### Serum stability testing

RNA–DNA hybrid nanoshapes were incubated for desired time with human serum at 3% concentration in 10 mM HEPES buffer, pH 7.0. Samples were analyzed by native PAGE.

## RESULTS AND DISCUSSION

### Design and assembly of the sandwich composite components

The nanotriangles were designed to contain modules partitioning architectural and functional roles between RNA and DNA components according to an approach that we recently established for nucleic acid hybrid nanoshapes (14,25). Self-assembling polygonal nanoshapes are obtained by combining autonomously folding RNA corner motifs as vectoring components with linear double-stranded DNA connectors that associate through short single-stranded complementary sequences. Here, a guide DNA with three hybridization sites ($DNA_{in}$) was used to assemble nanotriangles from RNA corner modules and DNA connectors ($DNA_{out}$) (Figure 1B). In such nanoshapes, association of nucleic acid modules directed by RNA fast folding kinetically favors the formation of circularly closed polygons over the slower end-to-end oligomerization (14). By introducing unique sequences in the hybridization sites of the DNA guide strand, the three DNA connector sides of a nanotriangle were programmed for successive assembly with biotin-conjugated oligonucleotides to furnish nanoshapes carrying 0–3 biotin ligands. Mobility analysis of the biotin-modified nanotriangles by native polyacrylamide gel electrophoresis (PAGE) confirmed the formation of clean RNA–DNA hybrid complexes (Figure 1C).

An initial attempt to prepare nano-sandwich complexes of streptavidin by mixing the protein with pre-assembled biotin-conjugated nanotriangles failed to deliver the desired architecture (Figure 2). Nanotriangles carrying a single biotin modification formed discrete complexes having a gel mobility consistent with 1–3 nucleic acid triangles bound to a streptavidin protein (Figure 2A, lane 2). Addition of a fourth triangle was not observed, possibly prevented by sterical hindrance. Streptavidin binding of nanotriangles that contained two or three biotin ligands led to mostly aggregation in addition to the formation of some

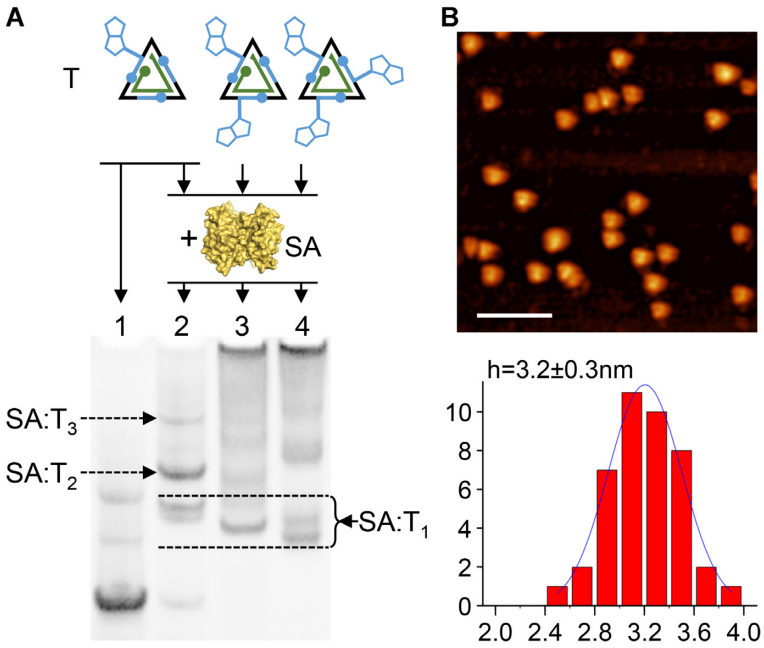


**Figure 2.** Complex formation of streptavidin with preformed nucleic acid nanotriangles. (**A**) PAGE analysis of mixtures that contained streptavidin tetramer protein (SA) and nucleic acid nanotriangles (T) carrying a defined number of biotin ligands. Nanotriangles with a single biotin modification formed complexes with 1–3 triangles bound to a single streptavidin tetramer (SA:$T_n$, $n = 1$–3). Nanotriangles conjugated with two or three biotin ligands formed equimolar complexes (SA:$T_1$) in addition to significant aggregation. Compaction of equimolar SA:$T_1$ assemblies by increasing number of biotin ligands that tether nanotriangles to streptavidin increased complex mobility. Double bands for equimolar SA:$T_1$ complexes observed with nanotriangles carrying one or three biotin ligands suggest formation of two different complex configurations due the non-equivalence of biotin binding sites on the protein tetramer. Lane 1 is a mobility control sample containing an RNA–DNA hybrid nanotriangle with a single biotin ligand. (**B**) AFM imaging of SA:$T_1$ complexes assembled from streptavidin and nanotriangles with two biotin ligands (panel A, lane 3). Scale bar, 50 nm. The histogram shows particle height measured by AFM which was consistent with equimolar complexes of a streptavidin tetramer positioned on top of a single RNA–DNA hybrid nanotriangle (14).

equimolar (SA:$T_1$) complex (Figure 2A, lanes 3, 4). Imaging and particle height measurements by atomic force microscopy (AFM) of purified equimolar (SA:$T_1$) complex between streptavidin bound to one nanotriangle with 2 biotin ligands (Figure 2A, lane 3) revealed the triangular shape of the nucleic acid component (Figure 2B) and supported the 1:1 stoichiometry of a streptavidin tetramer positioned on top of a single RNA–DNA hybrid nanotriangle (14).

We hypothesized that the failure of obtaining the nano-sandwich complex from the binding of preformed nanotriangles that carry two or three biotin ligands to streptavidin is caused by a kinetic effect that favors aggregation through crosslinking of proteins by nanotriangles. Following a fast association of the first biotin nanotriangle ligand with streptavidin, binding of the second conjugated biotin is kinetically disfavored through sterical hindrance which slows the favorable orientation of the nanoshape required for the formation of the second bond. Instead, association of the second biotin ligand with another streptavidin may become a competing reaction which eventually produces heterogeneous protein-nanotriangle aggregates.

### Multistep kinetic trapping assembly of the sandwich composite

To overcome the uncontrolled association of streptavidin and preformed nanotriangles ending in aggregates, we devised a synthetic route for the nano-sandwich that harnessed the rapid self-assembly of the RNA–DNA hybrid nanoshapes through short-range local interactions as a fast kinetic trap (26). We had previously demonstrated that RNA corner modules and DNA connectors that associate through hybridization of complementary single-stranded overhang sequences form exclusively polygonal nanoshapes without oligomerization or aggregate formation (14,25). During the folding and self-assembly of these nucleic acid hybrid architectures, incorporation of fast folding RNA modules provides precise vectoring of complementary sequences, thereby favoring the rapid formation of circularly closed nanoshapes over runaway oligomerization. To capitalize on the fast self-assembly of nanoshapes as a kinetic trap that prevents aggregation of the nano-sandwich components, we devised a stepwise synthetic route (II) in which the vectoring RNA corner modules are added last to a mixture of pre-formed protein-DNA and DNA precursor complexes (Figure 3A). Binding of biotin-conjugated $DNA_{out}$ connector oligonucleotides to streptavidin furnished a protein-DNA precursor complex for the sandwich core (Figure 3A, II-a) which was mixed with programmed guide $DNA_{in}$ and the complementary unmodified $DNA_{out}$ connector (Figure 3A, II-b). Addition of RNA corner module to the mixture of the protein–DNA and DNA precursors initiated rapid folding and self-assembly of the RNA–DNA hybrid nanoshapes at 37°C, which kinetically trapped the nucleic acid components in nanotriangles tethered at the protein sandwich core before association with further streptavidin tetramers occurred (Figure 3A, II-c). PAGE analysis of precursors and products

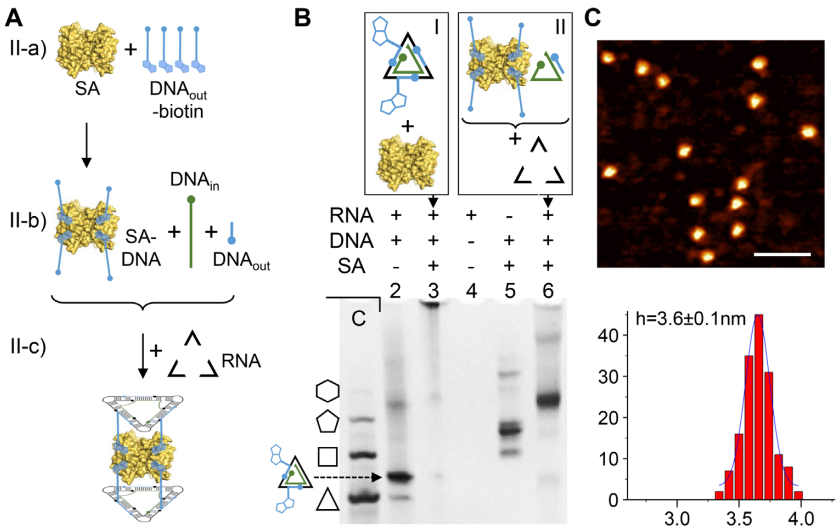


**Figure 3.** Synthesis of nucleic acid-streptavidin nano-sandwich composite. (**A**) Route II for kinetic-trapping assembly: II-a), binding of biotin-conjugated $DNA_{out}$ connector oligonucleotides to streptavidin (SA) furnishing the protein–DNA sandwich core complex precursor (SA-DNA); II-b), addition of $DNA_{in}$ guide and unmodified $DNA_{out}$ connector to the core complex precursor; II-c) induction of RNA–DNA hybrid nanotriangle self-assembly by addition of RNA corner modules. (**B**) PAGE analysis of precursors and products in synthetic routes for the nano-sandwich composite. In route I (shown also in Figure 2A, lane 3), preformed RNA–DNA hybrid nanotriangles carrying 2 biotin ligands (lane 2) are mixed with streptavidin which resulted in mostly aggregation (lane 3). Lane C is a mobility control sample containing a previously established mixture of polygonal RNA–DNA hybrid nanoshapes. In route II, a mixture containing preformed complex of biotin-conjugated DNA connectors bound to streptavidin (II-a) in addition to unconjugated DNA connector and DNA guide strand (II-b) was prepared first (lane 5). Subsequent addition of RNA corner modules furnished the nano-sandwich composite as a single predominant product (lane 6). (**C**) AFM imaging of the nano-sandwich composite product from gel lane 6 (scale bar, 50 nm). The histogram shows particle height measured by AFM.

of the kinetic-trapping route (II), in comparison with the route (I) of mixing pre-formed nanotriangles and streptavidin, demonstrated the synthesis of predominantly soluble nano-sandwich from route II in contrast to component aggregation in route I (Figure 3B). Clean formation of the nano-sandwich required close matching of the component stoichiometry to the expected 1:4 ratio of streptavidin tetramer to biotin-conjugated $DNA_{out}$ connector (Supplementary Figure S1). Aggregation at the expense of sandwich formation was observed with increasing concentration of the constituent components above a critical concentration, supporting the concept of kinetic trapping in the self-assembly process (Supplementary Figure S2).

Clean nano-sandwich complexes obtained through synthetic route II presented as discrete nanoparticles in AFM imaging (Figure 3C). To confirm the composition and structure of the nano-sandwich, we analyzed the product from synthetic route II by fluorescence labeling and cryo-EM (Figure 4). Incorporation of Cy5 acceptor dye-conjugated RNA corner module into the sandwich composite was monitored by Förster resonance energy transfer (FRET) with an Alexa 488 donor dye-labeled streptavidin protein. FRET signal was observed only when all components of the nano-sandwich were present but not when the dye-conjugated RNA and protein were mixed in the absence of DNA (Figure 4A), supporting the essential contribution of all constituents for the assembly of the sandwich architecture. When antisense DNA complementary to the biotin-conjugated $DNA_{out}$ connectors was added to fluorescent dye-labeled sandwich composite, the FRET signal decreased over time, which suggested dissociation of the sandwich architecture (Supplementary Figure S3).

## Cryo-EM imaging reveals the structure of the sandwich composite

Gel purification of nano-sandwich product obtained from synthetic route II provided a clean sample for structure analysis by cryo-EM (Figure 4A and B). Reconstruction of the 3D structure from particle imaging by cryo-EM confirmed the nano-sandwich architecture of the composite complex in agreement with the desired design (Figure 4D, Supplementary Figure S4). The shape and axial dimensions of the cryo-EM electron density map were consistent with a streptavidin protein core sandwiched between two nucleic acid nanotriangles in a staggered rotational arrangement. Height and diameter of the sandwich core density of 5 × 6 nm correspond closely to the dimensions of the streptavidin tetramer (27). The lateral width of the flanking triangle density at 6 nm was shorter, and the height at 3 nm larger than expected for the RNA–DNA hybrid nanotriangles (14). We hypothesized that the flexible attachment by two biotin-conjugated DNA strands at the streptavidin core allows for axial tilting mobility of the nanotriangles which led to a laterally compressed and axially extended envelope in the averaged density calculated from cryo-EM imaging (Supplementary Figure S5). While the axial tilting mobility of the nanoshapes may limit the resolution of the cryo-EM density map, the 3D reconstruction confirmed the architecture of the nano-sandwich and relative orientation of the nucleic acid triangles, and provided accurate overall dimensions. Future efforts on additional cryo-EM data collection of sandwich composite samples along with fitting of available crystal structures for the streptavidin protein and nucleic acid nanotriangle modules may lead to an atomic

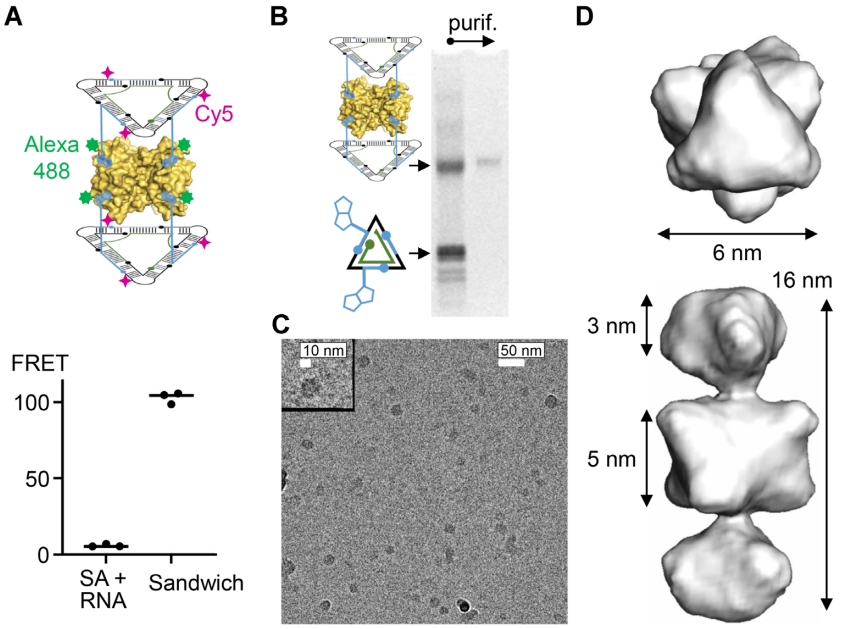


**Figure 4.** Structure characterization of nucleic acid-streptavidin nano-sandwich composite. (**A**) Nano-sandwich composite formation was demonstrated in solution by observing FRET signal from fluorescently labeled streptavidin (Alexa 488 donor dye) and RNA corner modules (Cy5 acceptor dye). Nano-sandwich composite prepared according to synthetic route II (Figure 3A) produced a robust signal whereas omission of DNA components abolished FRET. (**B**) Purification of nano-sandwich composite by native PAGE yielded a clean sample for structure determination by cryo-EM. (**C**) Representative electron micrograph of nano-sandwich composite sample. (**D**) Two orthogonal views of cryo-EM maps obtained by 3D reconstruction at ∼5.8 Å resolution under superimposed 3D symmetry for the nano-sandwich composite, shown as iso-density surface.

resolution model; however, any additional insight derived from such a high-resolution structure is likely to exceed only marginally the explanatory benefit of the current moderate-resolution density data that confirms the nano-sandwich architecture.

## CONCLUSIONS

The unique modular design of the nano-sandwich composite partitions architectural and functional roles between a protein as the central organizing core, RNA building blocks that undergo fast folding and provide precise vectoring for closed polygon formation, and DNA components that serve as connectors. In the proof-of-concept study presented here, assembly of the sandwich composite relied on the high-affinity interaction of streptavidin with biotin-conjugated DNA components in the nucleic acid nanoshapes. As we previously demonstrated, RNA–DNA hybrid nanoshapes provide a robust modular architecture that tolerates inclusion of diverse RNA corner and DNA connector units (14,25,28). To generalize the concept of the nano-sandwich composite model to other protein-nucleic acid systems, binding sites for single- or double-strand nucleic acid-binding proteins are readily engineered through sequence and topology modification of the connector modules (Figure 5A). This approach is applicable to both DNA- and RNA-binding proteins as either nucleic acid type may be used to introduce protein binding sites in lieu of the biotin-conjugated '$DNA_{out}$' connector strands used in this study (Figure 1B). Similar to the kinetic trapping assembly outlined for the streptavidin-based sandwich composite, formation of layered architectures from nucleic acid-binding proteins will commence with the preparation of a core precursor that consists of the protein in complex with connector nucleic acid containing the protein binding site (Figure 3A). The requirement for a stable core complex precursor that directs the kinetically fast association of subsequently added RNA corner modules limits the formation of nano-sandwich composites to proteins that bind nucleic acid with high (sub-micromolar) affinity. Preventing steric interference with sandwich formation directed by nucleic acid-binding proteins will require optimization of the linker sequence length between the connector component and the nucleic acid binding site (Figure 5A).

The modular architecture of the nanoshapes provides an opportunity to use nano-sandwich composites as repeating units for extended layered assemblies (29) through the introduction of RNA three-way junction (3WJ) folds as corner modules (Figure 5B). As we previously demonstrated (25), RNA 3WJ corner modules enable the lateral extension of nanoshapes via double-stranded connector DNA. The selection of modules in the nanoshape components of a sandwich composite can be programmed individually through sequence-encoded self-assembly of the building blocks.

Applications of nano-sandwich composites as individual units or as building blocks for extended materials include the creation of layered materials with precise control over protein arrangement and stoichiometry (8,30). As we envisage the use of nano-sandwich composites predominantly for *in vitro* and materials applications, we have not systematically assessed these nano-architectures for *in vivo* stability. Preliminary studies of the RNA–DNA hybrid nanoshape components in human serum suggest a half-life

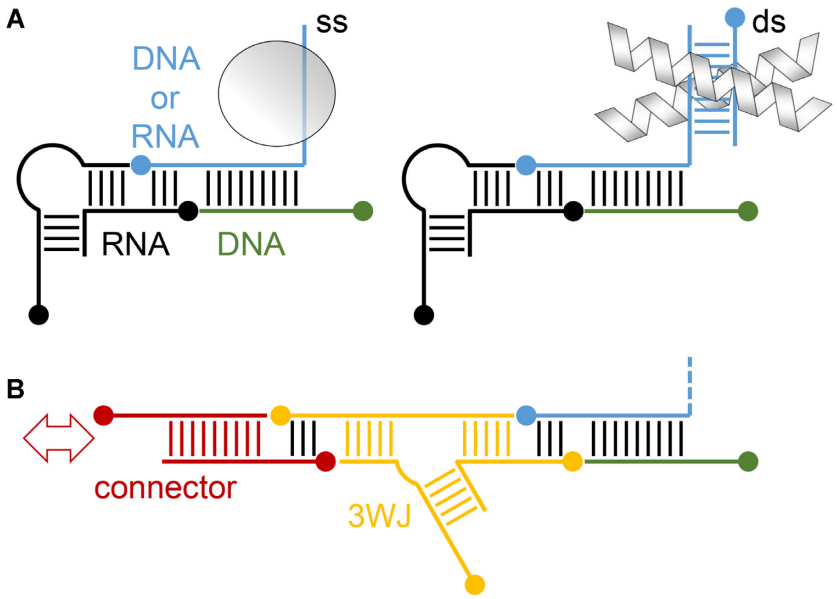


**Figure 5.** Modular design concepts for supramolecular sandwich architectures from protein, DNA and RNA components based on hybrid nanoshapes. (**A**) Proteins that recognize single- or double-stranded nucleic acid can be introduced by DNA or RNA components that contain protein binding sites in the modular connector modules (see Figure 1B) (14). (**B**) Extended materials can be obtained from sandwich composites by connecting nanoshapes containing RNA three-way junction (3WJ) corner motifs as we previously reported (25).

for the assemblies of >10 but <60 min (Supplementary Figure S6). For applications in biological milieu, nuclease resilience may be improved through chemical modification of the RNA components (31).

Nanoscale addressability of functional protein and nucleic acid components (30) in the composite material is achieved through the programmable spatial organization of the building blocks which is enabled through a high degree of cooperativity during the assembly process outlined here. Extended layers from the connection of nanosandwich composite units may have applications as materials carrying catalytic, sensor or molecular recognition functionality endowed by protein components and conjugates including enzymes, antibodies or constituent partners of protein-protein interaction pairs (8,30). Extended sandwich composite architectures may also serve as simplified, readily controllable synthetic frameworks for the in vitro study of complex interactions between protein components that require scaffolding by nucleic acid (8). Unlike the natural cognate ncRNA scaffolds, the synthetic composite frameworks can be engineered to contain a subset of protein binding sites enabling to explore the interaction of complex assemblies in a controlled fashion and by combinatorial approaches.

Taken together, the design concept and multistep synthesis strategy for the protein–RNA–DNA sandwich composite described here, combined with the versatility of robust nanoshape components, provide a general blueprint for the creation of extended composite materials that include alternating layers of proteins and nucleic acids which present diverse functional features embedded in patterns at the nanoscale. RNA–DNA hybrid nanoshapes which readily form under the control of fast folding RNA components provide powerful auxiliaries for nanomaterial formation under kinetic control.

## SUPPLEMENTARY DATA

Supplementary Data are available at NAR Online.

## ACKNOWLEDGEMENTS

The authors thank T. Wiryaman for help with analysis of cryo-EM data. The authors acknowledge the use of facilities and instrumentation at the UC Irvine Materials Research Institute (IMRI), which is supported in part by the National Science Foundation through the UC Irvine Materials Research Science and Engineering Center (grant DMR-2011967).

## FUNDING

UC San Diego Academic Senate [BG096646, in part]; National Science Foundation, Division of Materials Research [DMR-2104335]. Funding for open access charge: National Science Foundation (NSF).
*Conflict of interest statement.* None declared.

## REFERENCES

1. Westhof,E., Masquida,B. and Jaeger,L. (1996) RNA tectonics: towards RNA design. *Fold. Des.*, **1**, R78–R88.
2. Jaeger,L. and Chworos,A. (2006) The architectonics of programmable RNA and DNA nanostructures. *Curr. Opin. Struct. Biol.*, **16**, 531–543.
3. Ishikawa,J., Furuta,H. and Ikawa,Y. (2013) RNA tectonics (tectoRNA) for RNA nanostructure design and its application in synthetic biology. *WIRES RNA*, **4**, 651–664.
4. Seeman,N.C. and Sleiman,H.F. (2017) DNA nanotechnology. *Nat. Rev. Mater.*, **3**, 17068.
5. Jasinski,D., Haque,F., Binzel,D.W. and Guo,P. (2017) Advancement of the emerging field of RNA nanotechnology. *ACS Nano*, **11**, 1142–1164.

6. Ohno,H., Akamine,S. and Saito,H. (2018) RNA nanostructures and scaffolds for biotechnology applications. *Curr. Opin. Biotechnol.*, **58**, 53–61.
7. Seeman,N.C. (2020) DNA Nanotechnology at 40. *Nano Lett.*, **20**, 1477–1478.
8. McCluskey,J.B., Clark,D.S. and Glover,D.J. (2020) Functional applications of nucleic acid-protein hybrid nanostructures. *Trends Biotechnol.*, **38**, 976–989.
9. Zhou,K., Dong,J., Zhou,Y., Dong,J., Wang,M. and Wang,Q. (2019) Toward precise manipulation of DNA-Protein hybrid nanoarchitectures. *Small*, **15**, e1804044.
10. Zhang,C., Tian,C., Guo,F., Liu,Z., Jiang,W. and Mao,C. (2012) DNA-directed three-dimensional protein organization. *Angew. Chem. Int. Ed.*, **51**, 3382–3385.
11. Hernandez-Garcia,A. (2021) Strategies to build hybrid Protein-DNA nanostructures. *Nanomaterials*, **11**, 1332.
12. Shibata,T., Fujita,Y., Ohno,H., Suzuki,Y., Hayashi,K., Komatsu,K.R., Kawasaki,S., Hidaka,K., Yonehara,S., Sugiyama,H. *et al.* (2017) Protein-driven RNA nanostructured devices that function in vitro and control mammalian cell fate. *Nat. Commun.*, **8**, 540.
13. Osada,E., Suzuki,Y., Hidaka,K., Ohno,H., Sugiyama,H., Endo,M. and Saito,H. (2014) Engineering RNA-protein complexes with different shapes for imaging and therapeutic applications. *ACS Nano*, **8**, 8130–8140.
14. Monferrer,A., Zhang,D., Lushnikov,A.J. and Hermann,T. (2019) Versatile kit of robust nanoshapes self-assembling from RNA and DNA modules. *Nat. Commun.*, **10**, 608.
15. Ke,W., Hong,E., Saito,R.F., Rangel,M.C., Wang,J., Viard,M., Richardson,M., Khisamutdinov,E.F., Panigaj,M., Dokholyan,N.V. *et al.* (2019) RNA–DNA fibers and polygons with controlled immunorecognition activate RNAi, FRET and transcriptional regulation of NF-kappaB in human cells. *Nucleic Acids Res.*, **47**, 1350–1361.
16. Afonin,K.A., Viard,M., Martins,A.N., Lockett,S.J., Maciag,A.E., Freed,E.O., Heldman,E., Jaeger,L., Blumenthal,R. and Shapiro,B.A. (2013) Activation of different split functionalities on re-association of RNA–DNA hybrids. *Nat. Nanotechnol.*, **8**, 296–304.
17. Afonin,K.A., Desai,R., Viard,M., Kireeva,M.L., Bindewald,E., Case,C.L., Maciag,A.E., Kasprzak,W.K., Kim,T., Sappe,A. *et al.* (2014) Co-transcriptional production of RNA–DNA hybrids for simultaneous release of multiple split functionalities. *Nucleic Acids Res.*, **42**, 2085–2097.
18. Agarwal,S. and Franco,E. (2019) Enzyme-driven assembly and disassembly of hybrid DNA-RNA nanotubes. *J. Am. Chem. Soc.*, **141**, 7831–7841.
19. Vantomme,G. and Meijer,E.W. (2019) The construction of supramolecular systems. *Science*, **363**, 1396–1397.
20. Li,M., Zheng,M., Wu,S., Tian,C., Liu,D., Weizmann,Y., Jiang,W., Wang,G. and Mao,C. (2018) In vivo production of RNA nanostructures via programmed folding of single-stranded RNAs. *Nat. Commun.*, **9**, 2196.
21. Fu,J., Wang,Z., Liang,X.H., Oh,S.W., St Iago-McRae,E. and Zhang,T. (2020) DNA-scaffolded proximity assembly and confinement of multienzyme reactions. *To. Curr. Chem.*, **378**, 38.
22. Ge,Z., Gu,H., Li,Q. and Fan,C. (2018) Concept and development of framework nucleic acids. *J. Am. Chem. Soc.*, **140**, 17808–17819.
23. Parsons,J., Castaldi,M.P., Dutta,S., Dibrov,S.M., Wyles,D.L. and Hermann,T. (2009) Conformational inhibition of the hepatitis C virus internal ribosome entry site RNA. *Nat. Chem. Biol.*, **5**, 823–825.
24. Shlyakhtenko,L.S., Gall,A.A., Filonov,A., Cerovac,Z., Lushnikov,A. and Lyubchenko,Y.L. (2003) Silatrane-based surface chemistry for immobilization of DNA, protein-DNA complexes and other biological materials. *Ultramicroscopy*, **97**, 279–287.
25. Chen,S., Zhang,Z., Alforque,E. and Hermann,T. (2021) Complex RNA–DNA hybrid nanoshapes from iterative mix-and-match screening. *Nano Res.*, **14**, 46–51.
26. Yan,Y., Huang,J. and Tang,B.Z. (2016) Kinetic trapping - a strategy for directing the self-assembly of unique functional nanostructures. *Chem. Commun.*, **52**, 11870–11884.
27. Fan,X., Wang,J., Zhang,X., Yang,Z., Zhang,J.C., Zhao,L., Peng,H.L., Lei,J. and Wang,H.W. (2019) Single particle cryo-EM reconstruction of 52 kDa streptavidin at 3.2 Angstrom resolution. *Nat. Commun.*, **10**, 2386.
28. Chen,S. and Hermann,T. (2020) RNA–DNA hybrid nanoshapes that self-assemble dependent on ligand binding. *Nanoscale*, **12**, 3302–3307.
29. Geary,C., Chworos,A., Verzemnieks,E., Voss,N.R. and Jaeger,L. (2017) Composing RNA nanostructures from a syntax of RNA structural modules. *Nano Lett.*, **17**, 7095–7101.
30. Xia,K., Shen,J., Li,Q., Fan,C. and Gu,H. (2020) Near-atomic fabrication with nucleic acids. *ACS Nano*, **14**, 1319–1337.
31. Haque,F., Pi,F., Zhao,Z., Gu,S., Hu,H., Yu,H. and Guo,P. (2018) RNA versatility, flexibility, and thermostability for practice in RNA nanotechnology and biomedical applications. *WIRES RNA*, **9**, 1452.